



Title	Influence of implant length and diameter, bicortical anchorage, and sinus augmentation on bone stress distribution: Three-dimensional finite element analysis
Author(s)	Moriwaki, Hiroyoshi; Yamaguchi, Satoshi; Nakano, Tamaki et al.
Citation	International Journal of Oral and Maxillofacial Implants. 2016, 31(4), p. 84-91
Version Type	AM
URL	https://hdl.handle.net/11094/93080
rights	© 2016 by Quintessence Publishing Co Inc.
Note	

The University of Osaka Institutional Knowledge Archive : OUKA

<https://ir.library.osaka-u.ac.jp/>

The University of Osaka

1 Original Paper

2

3 **Influence of Implant Length and Diameter, Bicortical Anchorage, and Sinus**

4 **Augmentation on Bone Stress Distribution: Three-dimensional Finite Element Analysis**

5

6 Hiroyoshi Moriwaki, DDS; * Satoshi Yamaguchi, PhD; † Tamaki Nakano, DDS, PhD; *

7 Yasufumi Yamanishi, DDS, PhD; * Satoshi Imazato, DDS, PhD; † Hirofumi Yatani, DDS,

8 PhD*

9 ¹Department of Fixed Prosthodontics, Osaka University Graduate School of Dentistry,

10 1-8 Yamadaoka, Suita, Osaka 565-0871, Japan

11 ²Department of Biomaterials Science, Osaka University Graduate School of Dentistry,

12 1-8 Yamadaoka, Suita, Osaka 565-0871, Japan

13

14 Correspondence should be addressed to:

15 Satoshi Yamaguchi

16 Tel.: +81-6-6879-2919, Fax: +81-6-6879-2919

17 Email: yamagu@dent.osaka-u.ac.jp

18

19 No conflict of interest

20

1 ABSTRACT

2 Purpose: Clarification of the protocol for using short implants is required to enable
3 widespread use of short implants as an available treatment option. The purpose of this
4 study was to investigate the influences of implant length and diameter, bicortical
5 anchorage, and sinus augmentation on peri-implant cortical bone stress by
6 three-dimensional finite element analysis.

7 Materials and Methods: For bone models with bone quantity A and C in the maxillary
8 molar region, three-dimensional finite element analysis was performed using different
9 lengths and diameters of implant computer-aided design models, and the degree of
10 maximum principal stress distribution for each model was calculated.

11 Results: For bone quantity A models, the degree of stress distribution of 4-mm-diameter
12 and 6-mm-length implant was greatest. For bone quantity C models, the degree of
13 stress distribution of 5-mm-diameter and 6-mm-length implant with bicortical
14 anchorage was much smaller than that for 4-mm-diameter and 13-mm-length implant
15 with sinus augmentation.

16 Conclusions: Our results suggest that 6-mm-length implants should be selected in cases
17 with bone quantity C where the bone width permits increasing implant diameter from 4
18 mm to 5 mm.

1 Keywords: dental implants, sinus floor augmentation, biomechanics, finite element

2 analysis

3

ACCEPTED MANUSCRIPT

1 1. INTRODUCTION

2 Implant therapy has been applied to various clinical cases as a prosthetic treatment
3 option because of its positive clinical performance^{1, 2}. However, alveolar bone quantity
4 C³ caused by severe periodontal disease, and a long-term edentulous jaw⁴, restricts the
5 use of implant therapy. While bone augmentation such as sinus augmentation^{5, 6} and
6 veneer grafting^{7, 8}, and lateralization of the inferior alveolar nerve^{9, 10} are adopted to
7 allow insertion of implants, these therapies still have disadvantages such as surgical
8 invasion and infection, risks of sensory nerve paralysis, prolonged treatment time, and
9 an increase in treatment cost¹¹.

10 Meanwhile, short implants have achieved a significant market share owing to
11 the improvement in implant surface characteristics¹², and have been released by
12 various manufacturers. *In silico* study¹³ reported that there was no difference in
13 peri-implant bone stress caused by changing the length of the implant body when
14 measured by finite element analysis using simplified computer-aided design models.
15 Clinical studies have reported that the survival rates of standard length and short
16 implants were equivalent^{14, 15}. Recent clinical evidence has mentioned that the use of
17 short implants may be considered an alternative to more complicated bone
18 augmentation surgeries¹⁶. They have concluded that the use of short implants gives

1 patients lower risk, shorter clinical time, and decreased cost when compared with bone
2 augmentation surgeries¹⁷. These advantages of using short implants as compared with
3 bone augmentation surgeries were also mentioned in other studies¹⁸⁻²⁰ and there were
4 few differences in survival rate between short and standard length implants.

5 However, the risk for bone resorption in osseointegrated implants is greater for
6 treatment involving short implants⁸. Clinicians must follow certain protocols when
7 using short implants, e.g., splinting to other implants^{21, 22}, no use for single-tooth
8 replacement in molar sites²², and the use of wider diameter for short implants²¹. In
9 cases that cannot satisfy these protocols, bone augmentation surgery is selected,
10 especially in the maxilla.

11 The purpose of this study was to investigate the influences of implant length
12 and diameter, bicortical anchorage²³, and sinus augmentation on peri-implant cortical
13 bone stress using three-dimensional finite element analysis. For bone quantity A³ and C
14 models in the maxillary molar region, three-dimensional finite element analysis was
15 performed using two-piece implant computer-aided design models composed of an
16 implant body, abutment, and abutment screw.

17

1 2. MATERIALS AND METHODS

2 The models composed of an implant body, abutment, and abutment screw were created
3 using computer-aided design software (SolidWorks Premium 2011; SolidWorks
4 Corporation, Waltham, MA, USA) as shown in Fig. 1. The short-length and
5 regular-platform implant body was defined as $\phi 4 \times 6$ mm²⁴. The long length and regular
6 platform implant body was defined as $\phi 4 \times 13$ mm²⁴. The short-length and wide-platform
7 implant body was defined as $\phi 5 \times 6$ mm²⁴. The implant-abutment joints comprised an
8 internal joint. The pitch of threads with 0.66-mm intervals and the shape of the threads
9 were the same in all implants. The height of the abutment was 7.0 mm. The implant
10 and abutment were connected by the abutment screw.

11 Two computer-aided design models of posterior maxillary bone were created
12 with missing premolars and molars (Fig. 2). Alveolar bone quantity A and C models
13 were designed to enable insertion of implants 13.0 mm and 6.0 mm in length,
14 respectively. The overlying cortical bone of both models was designed to be 1.0 mm
15 thick^{12, 25}. The remaining areas were designed as cancellous bone.

16 The $\phi 4 \times 6$ mm, $\phi 4 \times 13$, and the $\phi 5 \times 6$ implants were placed on the bone quantity
17 A model (Fig. 3). Although not used in a clinical situation, these models were prepared
18 as controls to investigate the influence of implant length, bicortical anchorage, and

1 implant diameter. Similarly, 6-mm length implants were placed on the bone quantity C
2 model with bicortical anchorage (Fig. 4). The 13-mm length implant was placed on the
3 bone quantity C model with sinus augmentation, which was composed of maxillary bone
4 and graft materials (Fig. 5). As a control model, the $\phi 4 \times 6$ mm implant was placed on the
5 bone quantity C model with bicortical anchorage and sinus augmentation, and the
6 $\phi 4 \times 13$ mm implant was placed on the bone quantity C model without sinus
7 augmentation (Fig. 6).

8 The mechanical properties of bone, titanium, and the graft material used for
9 the three-dimensional finite element analysis²⁵⁻³⁰ are shown in Table 1. In this study,
10 the properties of the graft material were equalized for cancellous bone by assuming
11 100% substitution. For simulations of osseointegrated implants, a “fixed bond” condition
12 was set at the interface between the bone or graft material and the implant body²⁶. A
13 “contact” condition with a static friction coefficient of 0.2³¹, which accepts possible
14 microscopic sliding, was set at the interfaces among components of the implants²⁴. The
15 mesial and distal surfaces of the maxillary bone were fixed, and a static load of 150 N³²
16 was applied to the basal ridge surface of the abutment at 30° in a direction oblique to
17 the long axis of the implants³⁰ (Fig. 7). The elements for three-dimensional finite
18 element analysis were tetrahedrons with 16 nodes. To determine the mesh size that

1 offers an accurate result in a reasonable amount of computation time (less than 40 min),

2 the number of elements was increased until the maximum principal stress converged.

3 The results of convergence analysis³⁰ are shown in Table 2. The mesh size was

4 standardized to 0.3 mm in all models. Three-dimensional finite element analysis was

5 performed using the add-in function of the computer-aided design software.

6 The degree of maximum principal stress distribution to peri-implant cortical

7 bone, which was greater than or equal to the absolute value of the threshold, was

8 extracted using computer-aided design software (Fig. 8). The threshold for each value

9 obtained by three-dimensional finite element analysis was set once every 10 MPa from

10 -40 to 40 MPa.

11 To investigate the influence of implant length, bicortical anchorage, sinus

12 augmentation, and implant diameter, the degree of loss of maximum principal stress

13 distribution in four groups with: (A) different implant lengths ($\phi 4 \times 6$ mm implants

14 placed on the bone quantity A $\rightarrow \phi 4 \times 13$ mm implants placed on the bone quantity A,

15 $\phi 4 \times 6$ mm implants placed on the bone quantity C with sinus augmentation $\rightarrow \phi 4 \times 13$ mm

16 implants placed on the bone quantity C with sinus augmentation, and $\phi 4 \times 6$ mm

17 implants placed on the bone quantity C with bicortical anchorage $\rightarrow \phi 4 \times 13$ mm implants

18 placed on the bone quantity C with bicortical anchorage), (B) the implementation of

1 bicortical anchorage ($\phi 4 \times 6$ mm implants placed on the bone quantity A→ $\phi 4 \times 6$ mm
2 implants placed on the bone quantity C with bicortical anchorage, $\phi 4 \times 13$ mm
3 implants placed on the bone quantity A→ $\phi 4 \times 13$ mm implants placed on the bone
4 quantity C with bicortical anchorage), (C) the implementation of sinus augmentation
5 ($\phi 4 \times 6$ mm implants placed on the bone quantity C with bicortical anchorage→ $\phi 4 \times 6$ mm
6 implants placed on the bone quantity C with sinus augmentation, $\phi 4 \times 13$ mm implants
7 placed on the bone quantity C with bicortical anchorage→ $\phi 4 \times 13$ mm implants placed on
8 the bone quantity C with sinus augmentation), and (D) different implant diameters
9 ($\phi 4 \times 6$ mm implants placed on the bone quantity A→ $\phi 5 \times 6$ mm implants placed on the
10 bone quantity A, $\phi 4 \times 6$ mm implants placed on the bone quantity C with bicortical
11 anchorage→ $\phi 5 \times 6$ mm implants placed on the bone quantity C with bicortical
12 anchorage) were compared (Fig. 9).

1 3. RESULTS

2 3.1. *Degree of maximum principal stress distribution in peri-implant cortical bone*

3 Figure 10 shows the degree of maximum principal stress distribution in peri-implant

4 cortical bone for the bone quantity A model. The degree of maximum principal stress

5 distribution for $\phi 4 \times 6$ mm implants was greater than that for $\phi 4 \times 13$ mm implants (Fig.6 10A and Fig. 10B). The degree of maximum principal stress distribution for $\phi 5 \times 6$ mm7 implants was smaller than that for $\phi 4 \times 6$ mm implants (Fig. 10A and Fig. 10B). However,

8 the degree of compressive stress (negative value of the maximum principal stress)

9 distribution for $\phi 5 \times 6$ mm implants was greater than that for $\phi 4 \times 13$ mm implants (Fig.

10 10A), and the degree of tensile stress (positive value of the maximum principal stress)

11 distribution for $\phi 5 \times 6$ mm implants was smaller than that for $\phi 4 \times 13$ mm implants (Fig.

12 10B).

13 For the bone quantity C model, the degree of tensile stress distribution for

14 $\phi 5 \times 6$ mm implants with bicortical anchorage was much smaller than that for $\phi 4 \times 13$

15 mm implants with sinus augmentation (Fig. 11B), while the degree of compressive

16 stress distribution for $\phi 4 \times 6$ mm implants with bicortical anchorage was greater than17 that for $\phi 4 \times 13$ mm implants with sinus augmentation (Fig. 11A).

18

1 3.2. *Degree of loss of maximum principal stress distribution*2 Figure 12 shows the results of the degree of loss of maximum principal stress
3 distribution in each model.4 In terms of compressive stress distribution (Fig. 12A), the implant diameters
5 highly influenced the degree of loss of maximum principal stress distribution for all
6 thresholds. The implant lengths and the use of bicortical anchorage were similar among
7 thresholds of 20, 30, and 40 MPa. The decrease in maximum principal stress
8 distribution related to sinus augmentation was less when compared with the other
9 three factors.10 In terms of tensile stress distribution (Fig. 12B), the implant diameter again
11 highly influenced the degree of loss of maximum principal stress distribution, similar to
12 the compressive stress distribution, and the implementation of bicortical anchorage was
13 second in line.14
15

1 4. DISCUSSION

2 For $\phi 4 \times 13$ mm implants placed on the bone quantity A, the degree of maximum
3 principal stress distribution of the peri-implant cortical bone was reduced in comparison
4 with $\phi 4 \times 6$ mm implants placed on the bone quantity A. This result was caused by
5 obtaining a larger cancellous bone surface area in $\phi 4 \times 13$ mm implants placed on the
6 bone quantity A. Occlusal forces were dispersed within the cancellous bone holding the
7 implant. Therefore, stress distribution to the peri-implant cortical bone, causing
8 peri-implant bone resorption, decreased. For the same reason, the degree of maximum
9 principal stress distribution to the peri-implant cortical bone for $\phi 5 \times 6$ mm implants
10 placed on the bone quantity A was reduced in comparison with $\phi 4 \times 6$ mm implants
11 placed on the bone quantity A. In addition, the 5-mm-diameter implant could be well
12 stabilized by cancellous bone against occlusal loading along the long axis of the implant
13 because of the large surface area of the implant apex. On the basis of these factors, $\phi 5 \times 6$
14 mm implants placed on the bone quantity A showed an equivalent degree of compressive
15 stress distribution to $\phi 4 \times 13$ mm implants placed on the bone quantity A, and the degree
16 of tensile stress distribution for $\phi 5 \times 6$ mm implants placed on the bone quantity A was
17 smaller than that for $\phi 4 \times 13$ mm implants placed on the bone quantity A. The ultimate
18 strength of human bone under tension is lower than under compression³³. These results

1 suggest that the 5-mm-diameter implant may be resistant to bone resorption when
2 compared with the 4-mm-diameter implant.

3 It is thought that the degree of maximum principal stress distribution for
4 $\phi 4 \times 13$ mm implants placed on the bone quantity C with sinus augmentation increased
5 in comparison with that for $\phi 4 \times 6$ mm implants placed on the bone quantity C with
6 bicortical anchorage, because while $\phi 4 \times 6$ mm implants placed on the bone quantity C
7 with bicortical anchorage was only influenced by bicortical anchorage as a
8 stress-reducing factor, $\phi 4 \times 13$ mm implants placed on the bone quantity C with sinus
9 augmentation was influenced by the implant length in addition to bicortical anchorage.

10 The implementation of bicortical anchorage could reduce the stress on peri-implant
11 bone²⁷. The success rate doubled for monocortically anchored implants, especially in the
12 maxilla, in a prospective clinical short-term study of bicortical anchorage³⁴. On the basis
13 of these two factors, $\phi 4 \times 13$ mm implants placed on the bone quantity C with sinus
14 augmentation displayed a reduced degree of stress distribution. However, the degree of
15 stress distribution for $\phi 4 \times 6$ mm implants placed on the bone quantity C with bicortical
16 anchorage was less than that of $\phi 4 \times 6$ mm implants placed on the bone quantity A,
17 because the use of bicortical anchorage leads to the dispersion of occlusal forces to the
18 cortical bone at sinus floor. In a conventional finite element analysis study, the

1 placement of a $\phi 5 \times 6$ mm implant reduced stress on the peri-implant bone, causing a
2 large surface area of contact with the wide implant, and stiff cortical bone²⁹. They
3 concluded that the placement of $\phi 5 \times 6$ mm implants was more effective than that of
4 long-length implants with sinus augmentation in terms of treatment cost, treatment
5 length, and the risk of additional surgeries for patients³⁰. In this study, the degree of
6 maximum principal stress distribution for $\phi 5 \times 6$ mm implants placed on the bone
7 quantity C with bicortical anchorage was much smaller than that for $\phi 4 \times 13$ mm
8 implants placed on the bone quantity C with sinus augmentation. It is thought that the
9 combination of implant diameter and bicortical anchorage had a bigger influence in
10 reducing maximum principal stress distribution than implant length, implant diameter,
11 and sinus augmentation.

12 Considering that overloading is included as one of the causes of peri-implant
13 bone resorption, all results suggest that selecting a longer implant is clinically desirable
14 when there is alveolar bone quantity A. When the bone quantity C is present, $\phi 5 \times 6$ mm
15 implants may be useful in cases where the bone width remains sufficient to permit
16 increasing the implant diameter from 4.0 mm to 5.0 mm.

17 There are various treatment methods available to reduce the stress on
18 peri-implant bone. Nevertheless, there are few reports of the comparison among these

1 methods in terms of stress reduction. Thus, this comparison study is expected to clarify
2 the guideline for clinical implant treatment where an alveolar bone quantity C is
3 present. Additionally, the long-term prognosis of clinical implant treatment can be
4 expected as an outcome of this study. The degree of loss of maximum principal stress
5 distribution by increasing implant length and that by implementing bicortical
6 anchorage was similar. This is because the dispersion of the occlusal forces to the
7 cancellous bone caused by increasing implant length and the dispersion to the cortical
8 bone at the implant apex caused by implementing bicortical anchorage were equal.

9 A conventional finite element analysis study reported that extensive bone
10 augmentation by sinus augmentation reduced the stress on peri-implant bone³⁵. In this
11 study, the influence of sinus augmentation was less significant than implant length,
12 diameter, and bicortical anchorage. This occurred because the contact area with the
13 maxillary bone was not increased even if a longer implant was inserted after sinus
14 augmentation. Thus, much of the occlusal loading on the implant had spread to the
15 maxillary bone rather than the sinus augmentation graft material.

16 Implant diameter was a more influential design parameter of the implant for
17 stress on the peri-implant bone than implant length and thread shape, especially for
18 short implants³⁶. Additionally, the implant diameter influenced stress levels and the

1 wider diameter implant could help to reduce bone stress³⁷. In this study, the degree of
2 loss of maximum principal stress distribution by increasing implant diameter was much
3 higher than the effect of implant length, bicortical anchorage, and sinus augmentation.
4 This result is caused by obtaining strong support, which resists subsidence of implants,
5 and retention, which resists rolling of implants, as a result of increasing the contact
6 area with cortical bone, which has better mechanical strength properties when
7 compared with cancellous bone. The increase in implant length in this study was 7.0
8 mm. In comparison with 6- and 10-mm-length implants, the influence of bicortical
9 anchorage may become greater than the influence of implant length because the
10 increase in implant length is 4.0 mm. Analyses of implants of various lengths are
11 ongoing.

12 The lack of simulation of the inhomogeneous and isotropic material properties
13 of human bone and of the graft material is one of the limitations of the
14 three-dimensional finite element analysis in this study. In addition, the evaluation of
15 primary mechanical stability and secondary biologic stability³⁸ is not possible by static
16 three-dimensional finite element analysis without the simulation of bone-implant
17 interface using the various ratios of osseointegration in this study. However, our results
18 with homogeneous and isotropic material properties definitively clarified the influence

1 of implant length, bicortical anchorage, sinus augmentation, and implant diameter even

2 if these results were biased.

3

1 5. CONCLUSION

2 Our results suggest that 4-mm-diameter implants with increased length should be
3 selected to reduce the maximum principal stress of peri-implant cortical bone when
4 bone quantity A is available. When there is bone quantity C, 6-mm-length implants
5 should be selected if the bone width is sufficient to permit increasing the implant
6 diameter from 4.0 mm to 5.0 mm.

7 The 6-mm-length implants with bicortical anchorage have the potential to
8 become a useful treatment in achieving a reduced risk of surgical invasion, shortening
9 clinical time, and presenting a lower cost to patients.

10

11

1 Acknowledgment

2 This research was supported by Grants-in-Aid for Scientific Research (Nos. 24592955
3 and 15K11195) from the Japan Society for the Promotion of Science.

4

1 REFERENCES

2 1) Scholander S. A retrospective evaluation of 259 single-tooth replacements by the
3 use of Bränemark implants. *Int J Prosthodont* 1999;12:483-491.

4 2) Priest G. Single-tooth implants and their role in preserving remaining teeth: a
5 10-year survival study. *Int J Oral Maxillofac Implants* 1999;14:181-188.

6 3) Ribeiro-Rotta RF, Lindh C, Pereira AC, Rohlin M. Ambiguity in bone tissue
7 characteristics as presented in studies on dental implant planning and placement:
8 a systematic review. *Clin Oral Implants Res* 2011;22:789-801.

9 4) Pietrokovski J, Massler M. Alveolar ridge resorption following tooth extraction. *J
10 Prosthet Dent* 1967;17:21-7.

11 5) Wallace SS, Tarnow DP, Froum SJ, et al. Maxillary sinus elevation by lateral
12 window approach: evolution of technology and technique. *J Evid Based Dent Pract*
13 2012;12:161-171.

14 6) Boyne PJ. Augmentation of the posterior maxilla by way of sinus grafting
15 procedures: recent research and clinical observations. *Oral Maxillofac Surg Clin
16 North Am* 2004;16:19-31, v-vi.

17 7) Bedrossian E, Tawfils A, Aljianian A. Veneer grafting: a technique for
18 augmentation of the resorbed alveolus prior to implant placement. A clinical report.

1 Int J Oral Maxillofac Implants 2000;15:853-858.

2 8) McAllister BS, Haghishat K. Bone augmentation techniques. J Periodontol

3 2007;78:377-396.

4 9) Fernández Díaz JÓ, Naval Gías L. Rehabilitation of edentulous posterior atrophic

5 mandible: inferior alveolar nerve lateralization by piezotome and immediate

6 implant placement. Int J Oral Maxillofac Surg 2013;42:521-526.

7 10) Peleg M, Mazor Z, Chaushu G, Garg AK. Lateralization of the inferior alveolar

8 nerve with simultaneous implant placement: a modified technique. Int J Oral

9 Maxillofac Implants 2002;17:101-106.

10 11) Friberg B, Gröndahl K, Lekholm U, Bränemark PI. Long-term follow-up of severely

11 atrophic edentulous mandibles reconstructed with short Bränemark implants. Clin

12 Implant Dent Relat Res 2000;2:184-189.

13 12) Wennerberg A, Albrektsson T. Effects of titanium surface topography on bone

14 integration: a systematic review. Clin Oral Implants Res 2009;20 Suppl 4:172-184.

15 13) Pierrisnard L, Renouard F, Renault P, Barquins M. Influence of implant length and

16 bicortical anchorage on implant stress distribution. Clin Implant Dent Relat Res

17 2003;5:254-262.

18 14) Mertens C, Meyer-Bäumer A, Kappel H, Hoffmann J, Steveling HG. Use of 8-mm

1 and 9-mm implants in atrophic alveolar ridges: 10-year results. *Int J Oral*
2 *Maxillofac Implants* 2012;27: 1501-1508.

3 15) Anitua E, Orive G. Short implants in maxillae and mandibles: A retrospective study
4 with 1 to 8 years of follow-up. *J Periodontol* 2010;81:819-826.

5 16) Renouard F, Nisand D. Short implants in the severely resorbed maxilla: a 2-year
6 retrospective clinical study. *Clin Implant Dent Relat Res* 2005;7:S104-110.

7 17) das Neves FD, Fones D, Bernardes SR, do Prado CJ, Neto AJ. Short implants--an
8 analysis of longitudinal studies. *Int J Oral Maxillofac Implants* 2006;21:86-93.

9 18) Monje A, Chan HL, Fu JH, Suarez F, Galindo-Moreno P, Wang HL. Are short dental
10 implants (<10 mm) effective? a meta-analysis on prospective clinical trials. *J*
11 *Periodontol* 2013;84:895-904.

12 19) Esposito M, Grusovin MG, Rees J, et al. Interventions for replacing missing teeth:
13 augmentation procedures of the maxillary sinus. *Cochrane Database Syst Rev*
14 2010;17;CD008397.

15 20) Sánchez-Garcés MA, Costa-Berenguer X, Gay-Escoda C. Short implants: a
16 descriptive study of 273 implants. *Clin Implant Dent Relat Res* 2012;14:508-16.

17 21) Romeo E, Bivio A, Mosca D, Scanferla M, Ghisolfi M, Storelli S. The use of short
18 dental implants in clinical practice: literature review. *Minerva Stomatol*

1 2010;59:23-31.

2 22) Buser D, von Arx T, ten Bruggenkate C, Weingart D. Basic surgical principles with
3 ITI implants. *Clin Oral Implants Res* 2000;11 Suppl 1:59-68.

4 23) Malo P, de Araujo Nobre M, Lopes A, Moss S. Posterior maxillary implants inserted
5 with bicortical anchorage and placed in immediate function for partial or complete
6 edentulous rehabilitations. A retrospective clinical study with a median follow-up of
7 7 years. *Oral Maxillofac Surg* 2015;19:19-27.

8 24) Noda K, Arakawa H, Kimura-Ono A, Yamazaki S, Hara ES, Sonoyama W, Maekawa
9 K, Okura K, Shintani A, Matsuka Y, Kuboki T. A longitudinal retrospective study of
10 the analysis of the risk factors of implant failure by the application of generalized
11 estimating equations. *J Prosthodont Res* 2015;59:178-84.

12 25) Abu-Hammad O, Khraisat A, Dar-Odeh N, El-Maaytah M. Effect of dental implant
13 cross-sectional design on cortical bone structure using finite element analysis. *Clin
14 Implant Dent Relat Res* 2007;9:217-21.

15 26) Yamanishi Y, Yamaguchi S, Imazato S, Nakano T, Yatani H. Influences of implant
16 neck design and implant-abutment joint type on peri-implant bone stress and
17 abutment micromovement: three-dimensional finite element analysis. *Dent Mater*
18 2012;28:1126-1133.

1 27) Huang HL, Fuh LJ, Ko CC, Hsu JT, Chen CC. Biomechanical effects of a maxillary
2 implant in the augmented sinus: a three-dimensional finite element analysis. *Int J*
3 *Oral Maxillofac Implants* 2009;24:455-62.

4 28) Pessoa RS, Vaz LG, Marcantonio E Jr, Vander Sloten J, Duyck J, Jaecques SV.
5 Biomechanical evaluation of platform switching in different implant protocols:
6 computed tomography-based three-dimensional finite element analysis. *Int J Oral*
7 *Maxillofac Implants* 2010;25:911-919.

8 29) Inglam S, Suebnukarn S, Tharanon W, Apatananon T, Sitthiseripratip K. Influence
9 of graft quality and marginal bone loss on implants placed in maxillary grafted
10 sinus: a finite element study. *Med Biol Eng Comput* 2010;48:681-689.

11 30) Chang SH, Lin CL, Lin YS, Hsue SS, Huang SR. Biomechanical comparison of a
12 single short and wide implant with monocortical or bicortical engagement in the
13 atrophic posterior maxilla and a long implant in the augmented sinus. *Int J Oral*
14 *Maxillofac Implants* 2012;27:e102-111.

15 31) Bulaqi HA, Mousavi Mashhadi M, Geramipanah F, Safari H, Paknejad M. Effect of
16 the coefficient of friction and tightening speed on the preload induced at the dental
17 implant complex with the finite element method. *J Prosthet Dent* 2015;113:405-411.

18 32) Ding X, Liao SH, Zhu XH, Zhang XH, Zhang L. Effect of diameter and length on

1 stress distribution of the alveolar crest around immediate loading implants. Clin
2 Implant Dent Relat Res 2009;11:279-287.

3 33) Reilly DT, Burstein AH. The elastic and ultimate properties of compact bone tissue.
4 J Biomech 1975;8:393-405.

5 34) Hessling K-H, Neukam FW, Scheller H, Günay H, Schmelzeisen R. Die extreme
6 Atrophie des Ober- und Unterkiefers. Klinische Gesichtspunkte bei der
7 Versorgung mit enossalen Implantaten. Z Zahnärztl Implantol 1990;6:35-39.

8 35) Tepper G, Haas R, Zechner W, Krach W, Watzek G. Three-dimensional finite
9 element analysis of implant stability in the atrophic posterior maxilla: a
10 mathematical study of the sinus floor augmentation. Clin Oral Implants Res
11 2002;13:657-665.

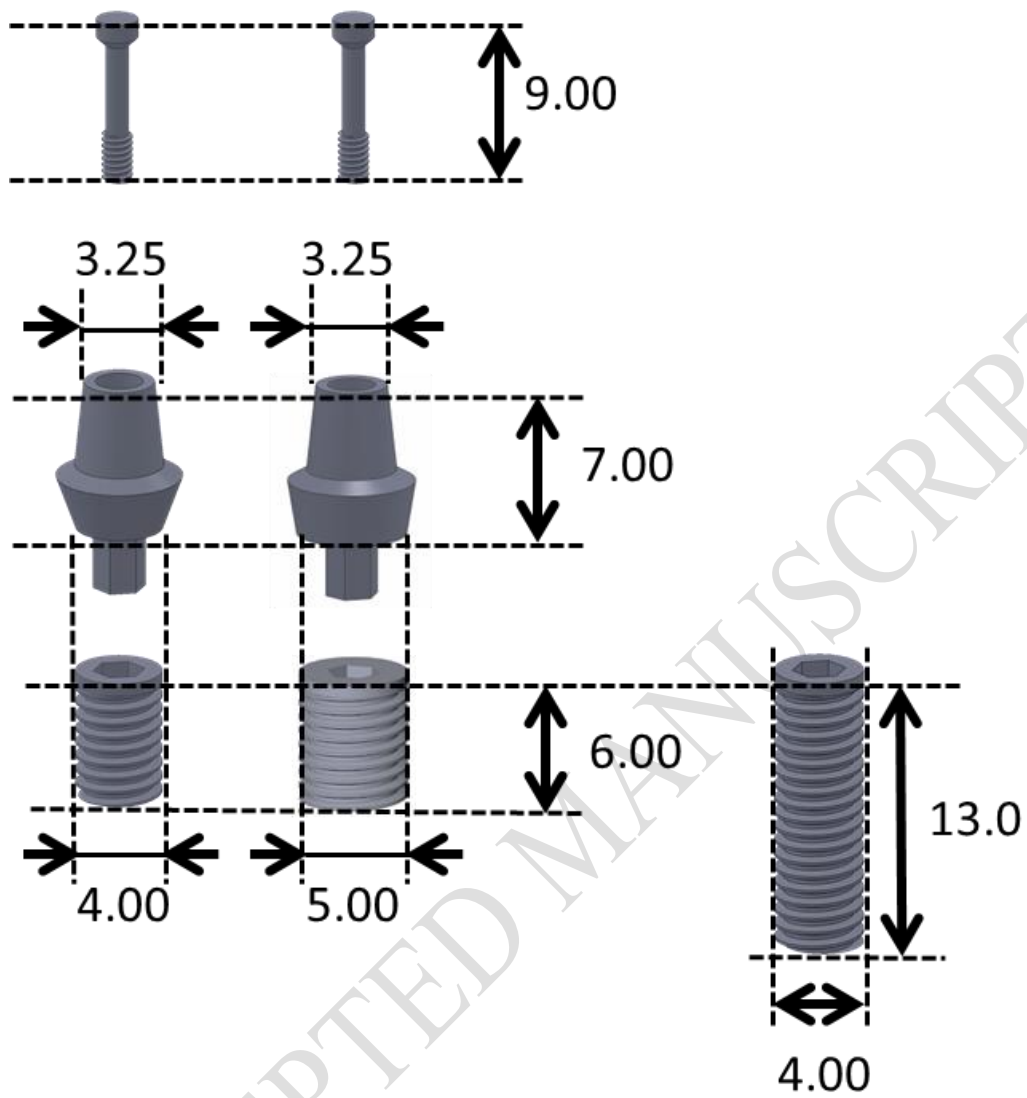
12 36) Vairo G, Sannino G. Comparative evaluation of osseointegrated dental implants
13 based on platform-switching concept: influence of diameter, length, thread shape,
14 and in-bone positioning depth on stress-based performance. Comput Math Methods
15 Med 2013;doi:10.1155/2013/250929.

16 37) Ormianer Z, Ben Amar A, Duda M, Marku-Cohen S, Lewinstein I. Stress and strain
17 patterns of 1-piece and 2-piece implant systems in bone: a 3-dimensional finite
18 element analysis. Implant Dent 2012;21:39-45.

1 38) Queiroz TP, Aguiar SC, Margonar R, de Souza Faloni AP, Gruber R, Luvizuto ER.
2 Clinical study on survival rate of short implants placed in the posterior mandibular
3 region: resonance frequency analysis. Clin Oral Implants Res 2014; doi:
4 10.1111/clr.12394.

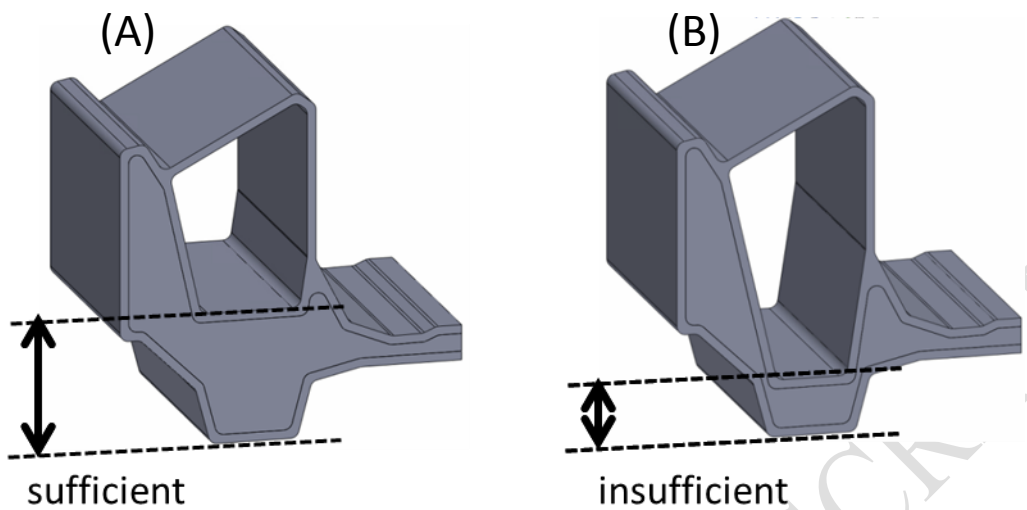
5 FIGURES

6 Fig. 1

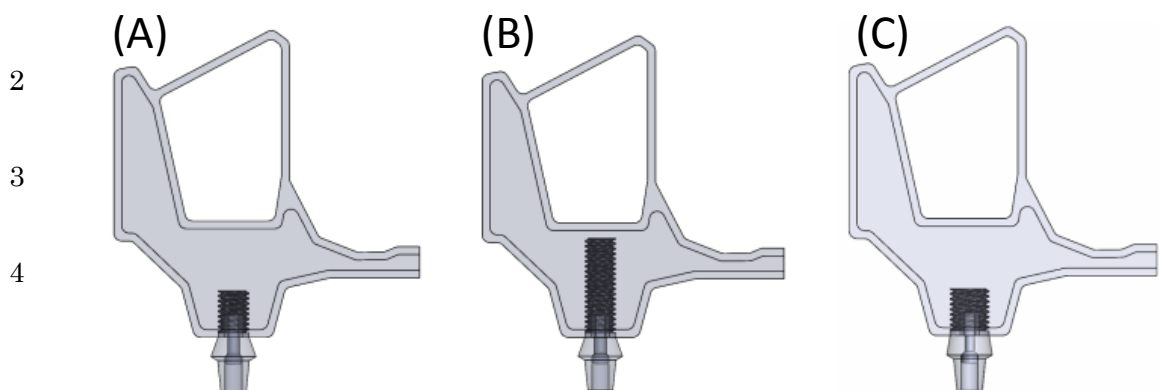


1
2
3
4

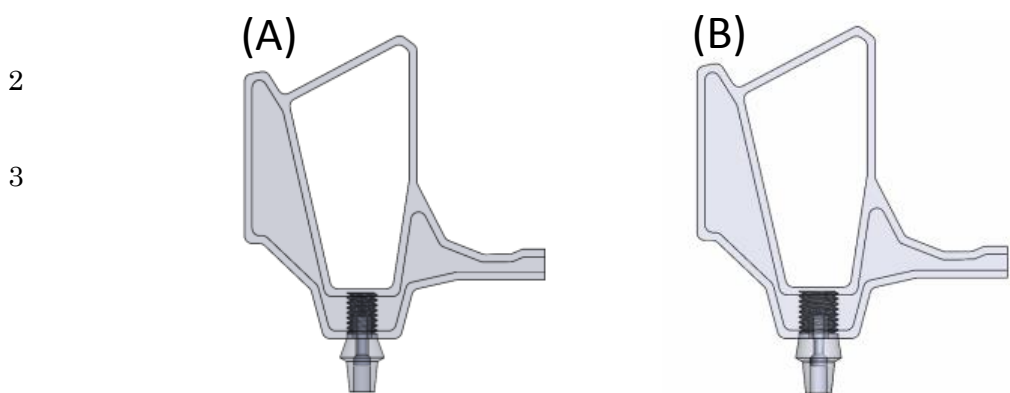
1 Fig. 2



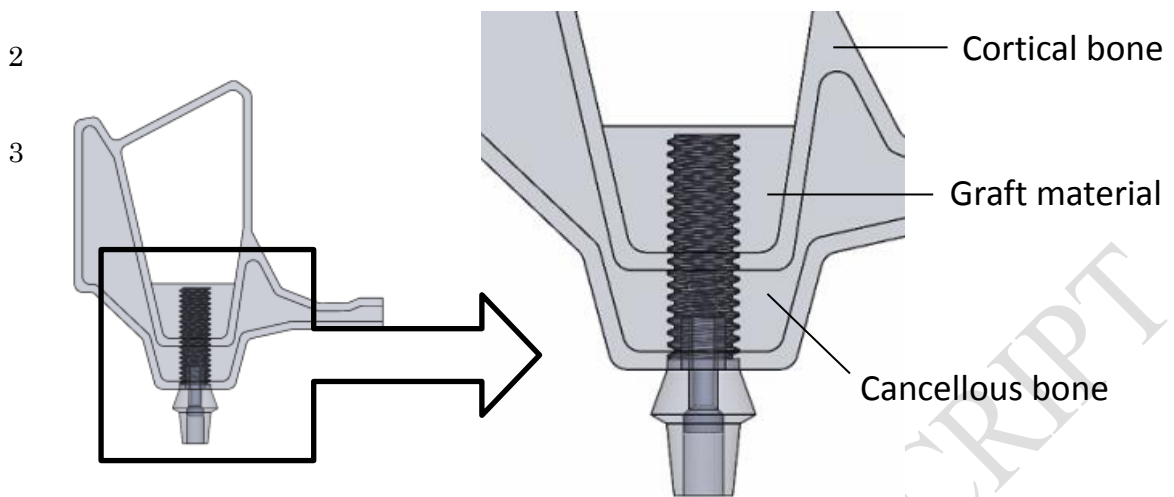
1 Fig. 3



1 Fig. 4

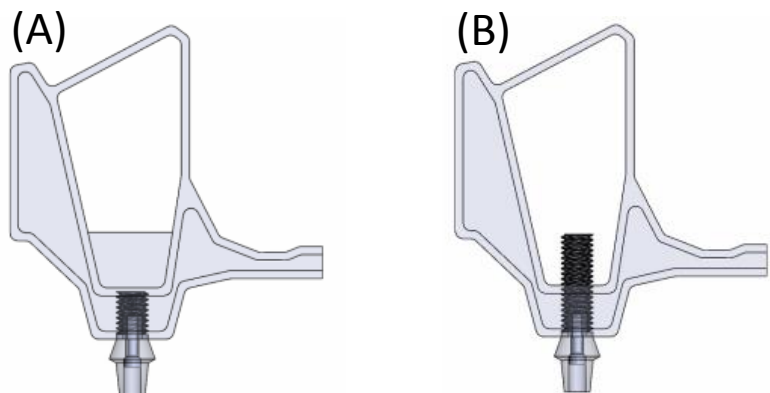


1 Fig. 5

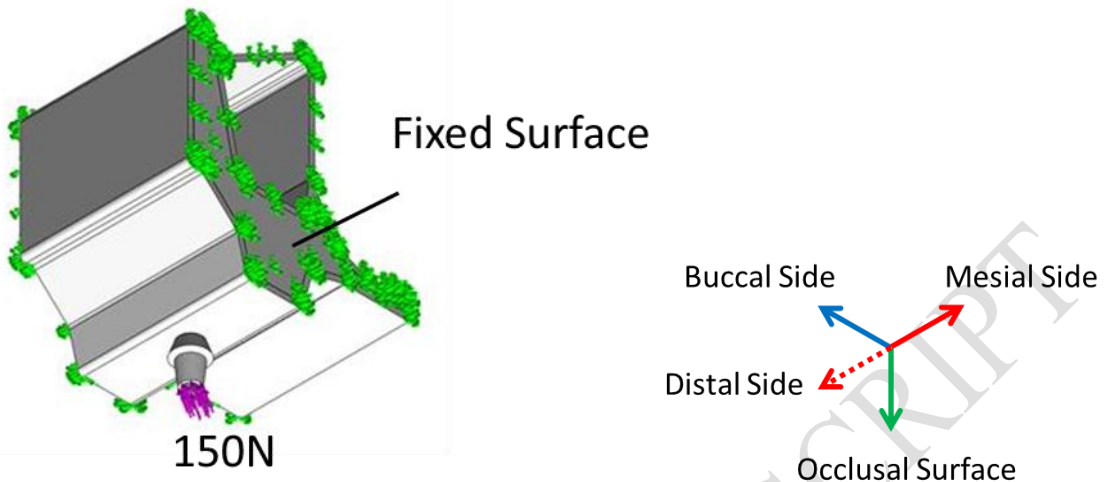


1 Fig. 6

2



1 Fig. 7

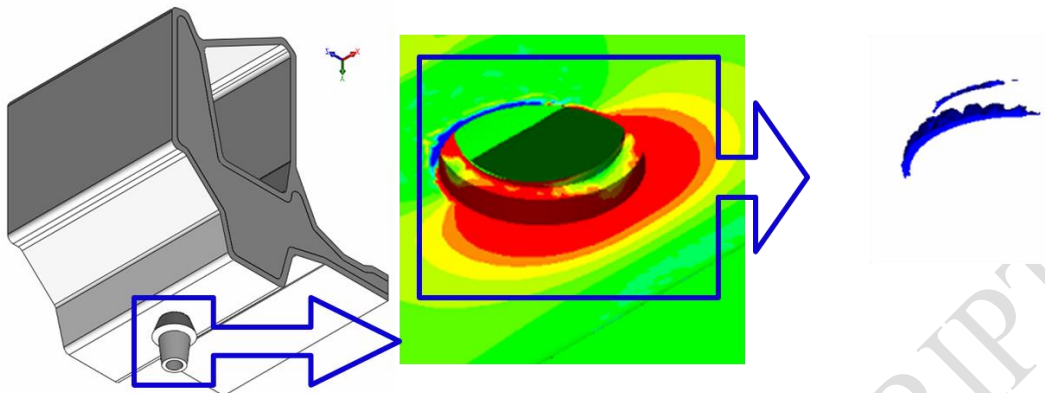


2

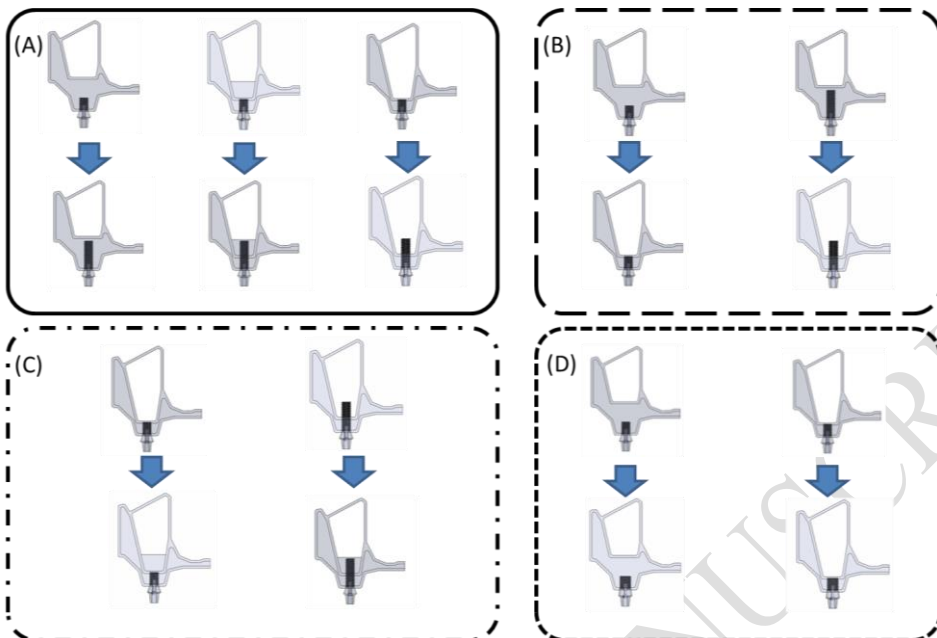
3

4

1 Fig. 8



1 Fig. 9



1 Fig. 10A

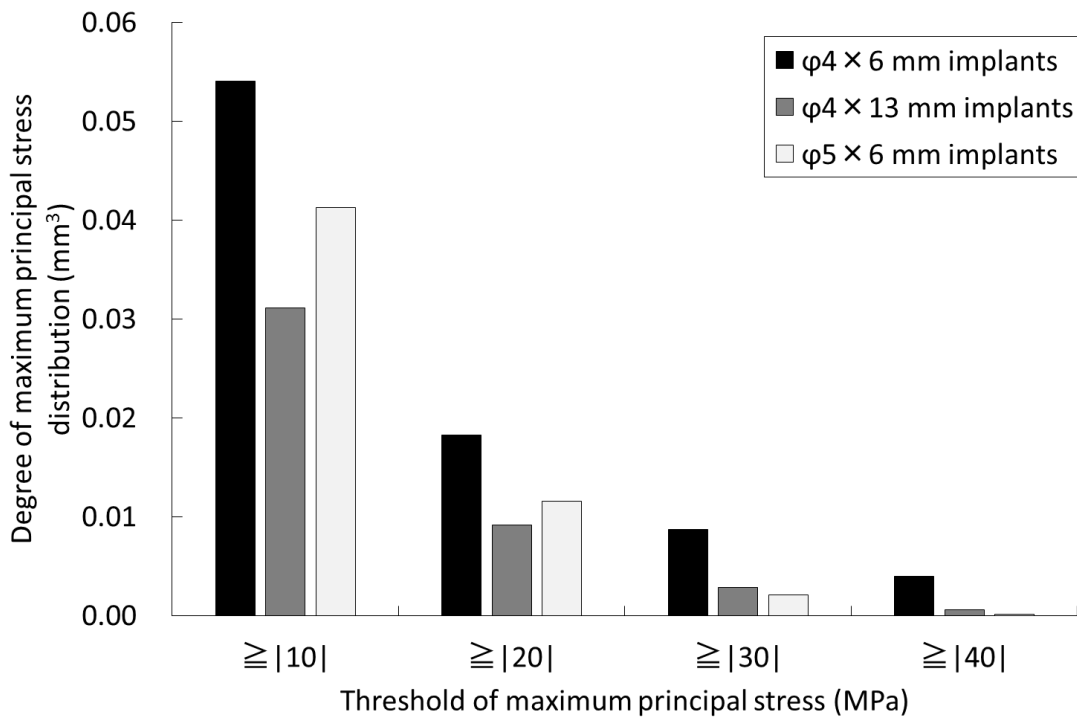
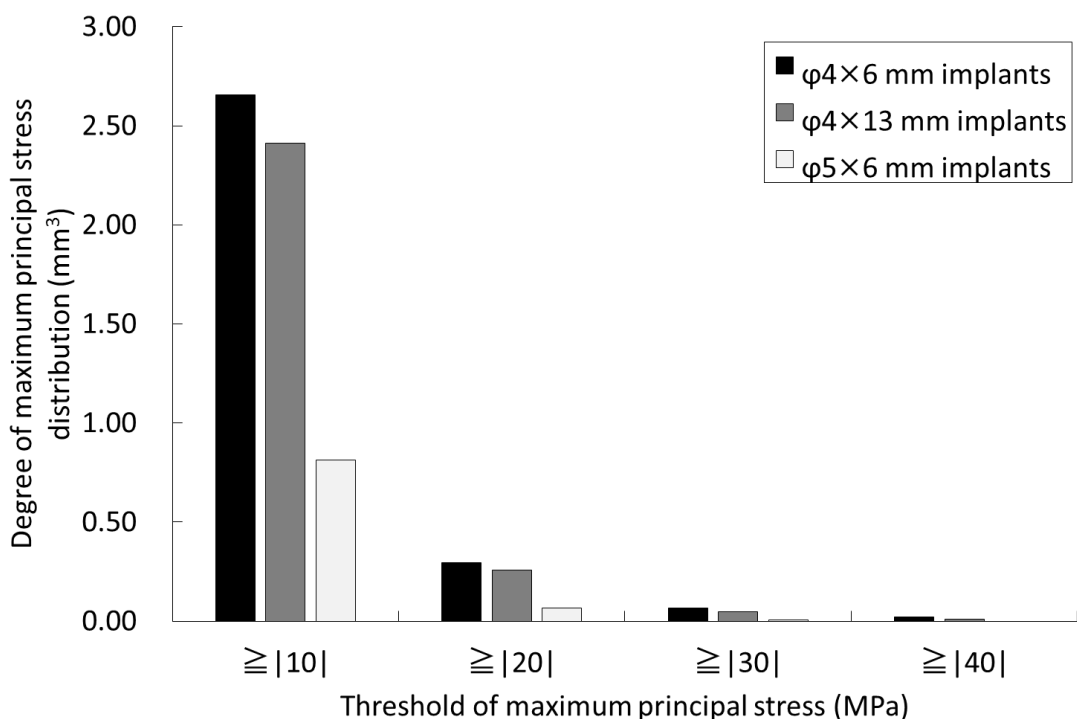


Fig. 10B



1 Fig. 11A

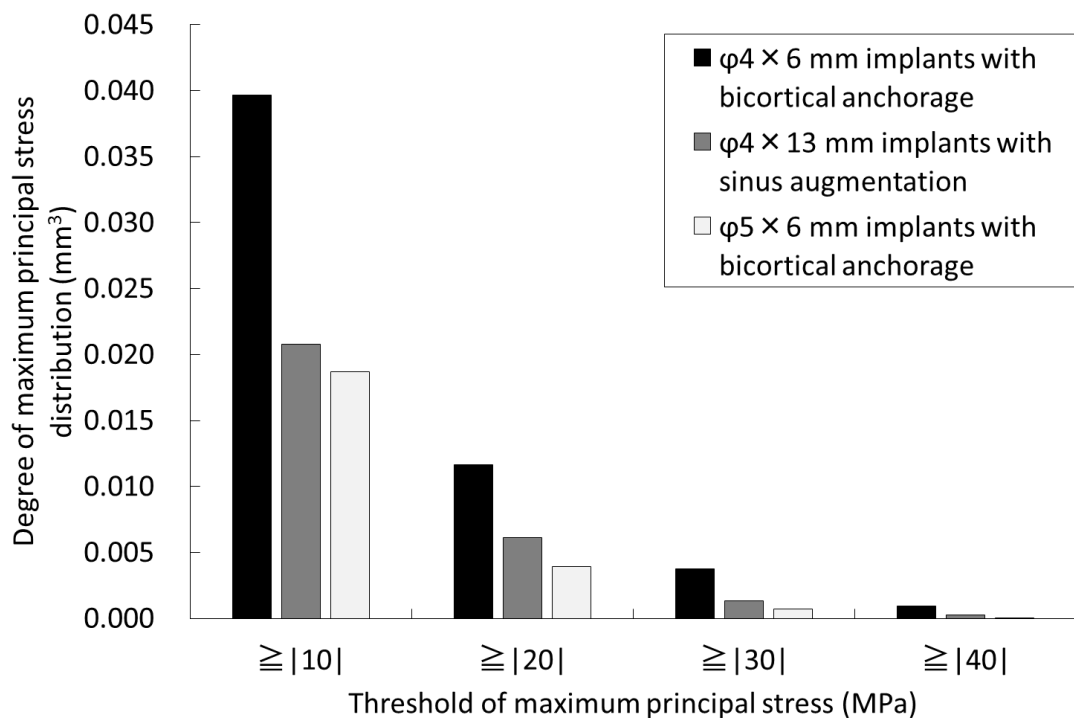
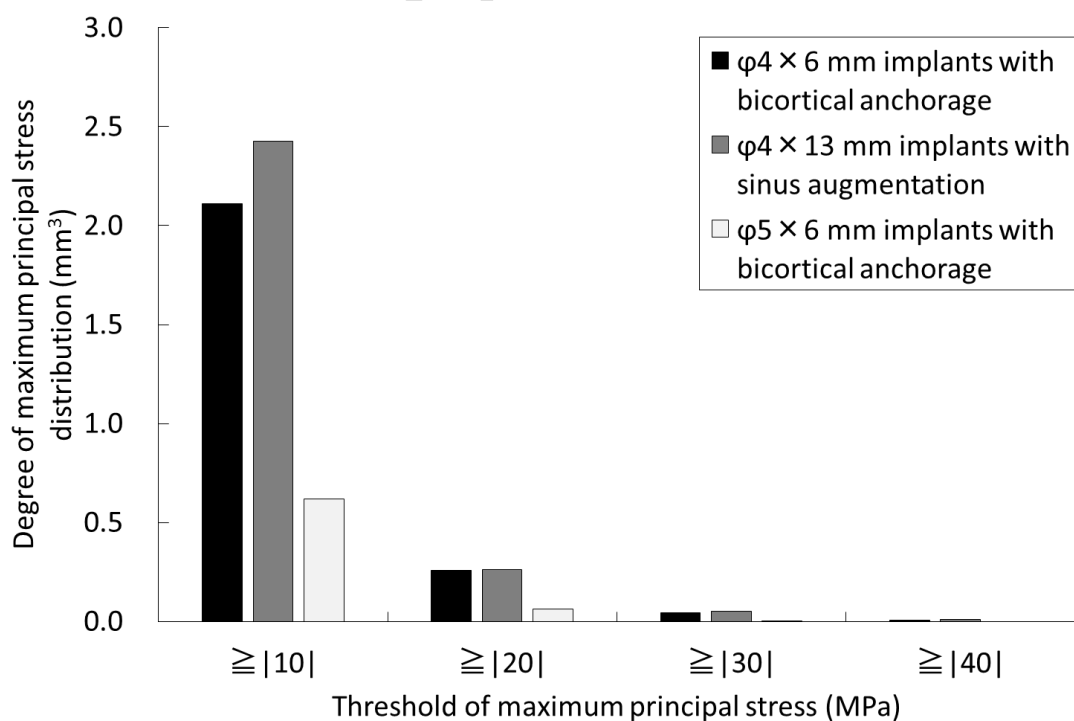
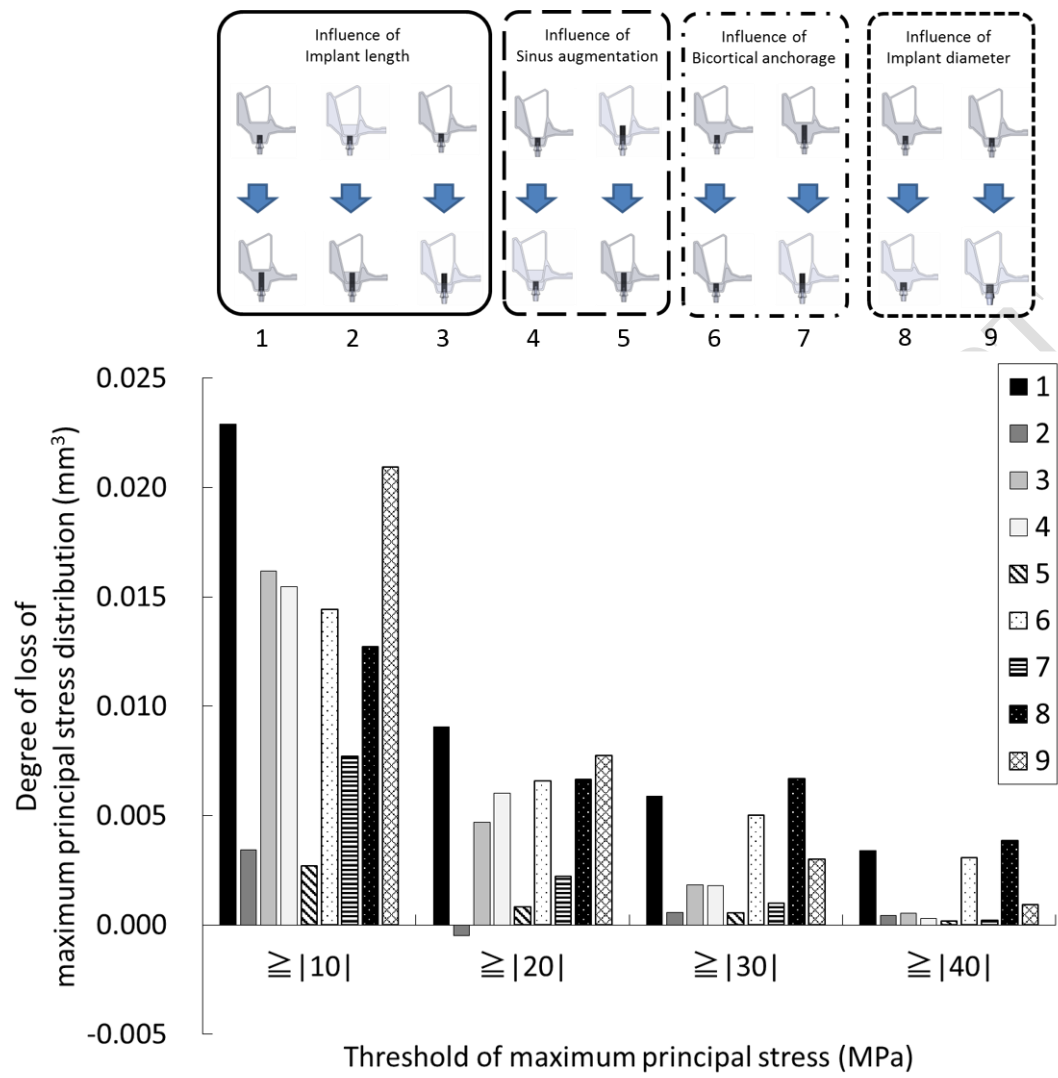


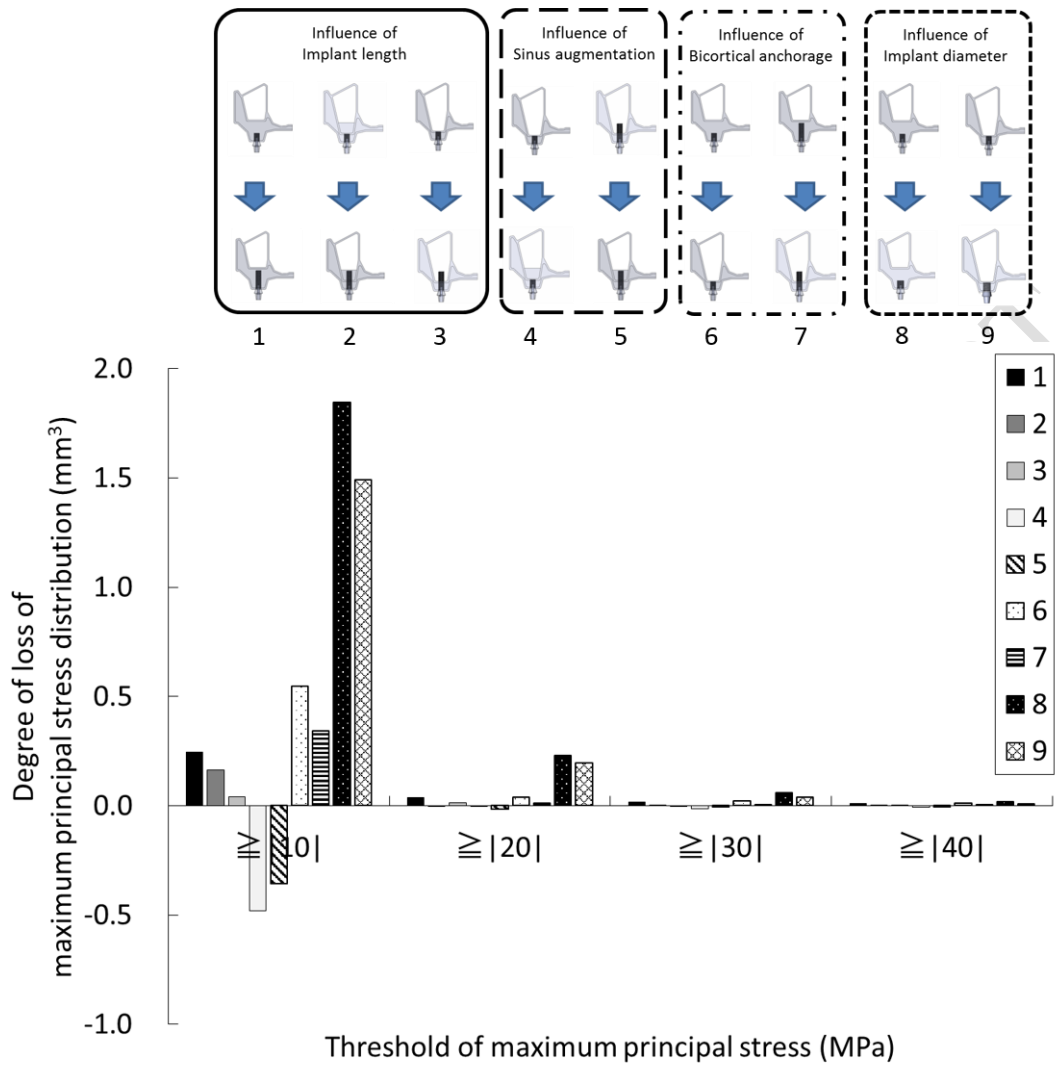
Fig. 11B



1 Fig. 12A

2
3

1 Fig. 12B



2

3

1 Table 1: Mechanical properties of each component used for finite element analysis

Components	Young's Moduli (MPa)	Poisson's Ratios
Cortical bone	13,000	0.3
Cancelloous bone	1,370	0.3
Implant components	117,000	0.3
Graft material	1,370	0.3

2

3

4

1 Table 2: Total numbers of elements for each model. 1. $\phi 4 \times 6$ mm implants, 2. $\phi 4 \times 13$ mm
2 implants, 3. $\phi 4 \times 6$ mm implants with bicortical anchorage, 4. $\phi 4 \times 13$ mm implants with
3 sinus augmentation, 5. $\phi 5 \times 6$ mm implants, 6. $\phi 5 \times 6$ mm implants with bicortical
4 anchorage, 7. $\phi 4 \times 6$ mm implants with bicortical anchorage and sinus augmentation, 8.
5 $\phi 4 \times 13$ mm implants without sinus augmentation.

	1	2	3	4	5	6	7	8
total								
number of elements	155,499	163,406	146,609	154,254	156,322	146,249	152,438	147,545

1 FIGURE LEGENDS

2

3 Fig. 1: Geometry of computer-aided design models of $\phi 4 \times 6$ mm implant (left), $\phi 5 \times 6$ mm
4 implant (middle), and $\phi 4 \times 13$ mm implant (right) (mm).

5

6 Fig. 2: Computer-aided design models of maxillary alveolar bone. (A) Bone quantity A.
7 (B) Bone quantity C.

8

9 Fig. 3: Computer-aided design models of each implant in the case of bone quantity A. (A)
10 $\phi 4 \times 6$ mm implants. (B) $\phi 4 \times 13$ mm implants. (C) $\phi 5 \times 6$ mm implants.

11

12 Fig. 4: Computer-aided design models of each implant in the case of bone quantity C. (A)
13 $\phi 4 \times 6$ mm implants with bicortical anchorage. (B) $\phi 5 \times 6$ mm implants with bicortical
14 anchorage.

15

16 Fig. 5: One of the computer-aided design models of each implant in the case of bone
17 quantity C with sinus augmentation, which was composed of maxillary bone and graft
18 materials.

1

2 Fig. 6: Two control models were prepared for comparing the influences of implant length
3 and diameter, bicortical anchorage, and sinus augmentation. (A) $\phi 4 \times 6$ mm implants
4 placed on the bone quantity C with bicortical anchorage and sinus augmentation. (B)
5 $\phi 4 \times 13$ mm implants placed on the bone quantity C without sinus augmentation.

6

7 Fig. 7: Assembled computer-aided design model of bone and implant models. The mesial
8 and distal section surfaces of the bone were fixed. Static load of 150 N was applied to the
9 basal ridge surface of the abutment at 30° in a direction oblique to the long axis of the
10 implants.

11

12 Fig. 8: Calculation procedure of the degree of maximum principal stress distributed to
13 peri-implant cortical bone. The maximum principal stress distribution to peri-implant
14 cortical bone greater than or equal to the absolute value of the threshold was extracted
15 by computer-aided design software. Total volume of extracted parts was calculated.

16

17 Fig. 9: Influence of four factors; implant length, bicortical anchorage, sinus
18 augmentation, and implant diameter.

1

2 Fig. 10: Degree of stress distribution in the bone quantity A model for $\phi 4 \times 6$ mm
3 implants, $\phi 4 \times 13$ mm implants, and $\phi 5 \times 6$ mm implants (mm^3), (A) Compressive stress,
4 (B) Tensile stress.

5

6 Fig. 11: Degree of stress distribution in the bone quantity C model for $\phi 4 \times 6$ mm
7 implants with bicortical anchorage, $\phi 4 \times 13$ mm implants with sinus augmentation, and
8 $\phi 5 \times 6$ mm with bicortical anchorage (mm^3), (A) Compressive stress, (B) Tensile stress.

9

10 Fig. 12: Degree of loss of compressive and tensile stress distribution (mm^3). 1. $\phi 4 \times 6$ mm
11 implants placed on the bone quantity A $\rightarrow \phi 4 \times 13$ mm implants placed on the bone
12 quantity A, 2. $\phi 4 \times 6$ mm implants with bicortical anchorage and sinus augmentation on
13 the bone quantity C $\rightarrow \phi 4 \times 13$ mm implants with sinus augmentation on the bone
14 quantity C, 3. $\phi 4 \times 6$ mm implants with bicortical anchorage on the bone quantity
15 C $\rightarrow \phi 4 \times 13$ mm implants without sinus augmentation on the bone quantity C, 4. $\phi 4 \times 6$
16 mm implants with bicortical anchorage on the bone quantity C $\rightarrow \phi 4 \times 6$ mm implants
17 with bicortical anchorage and sinus augmentation on the bone quantity C, 5. $\phi 4 \times 13$ mm
18 h implants without sinus augmentation on the bone quantity C $\rightarrow \phi 4 \times 13$ mm implants

- 1 with sinus augmentation on the bone quantity C, 6. $\phi 4 \times 6$ mm implants on the bone
- 2 quantity A $\rightarrow \phi 4 \times 6$ mm implants with bicortical anchorage on the bone quantity C. 7.
- 3 $\phi 4 \times 13$ mm implants on the bone quantity A $\rightarrow \phi 4 \times 13$ mm implants without sinus
- 4 augmentation on the bone quantity C, 8. $\phi 4 \times 6$ mm implants on the bone quantity
- 5 A $\rightarrow \phi 5 \times 6$ mm implants on the bone quantity A, 9. $\phi 4 \times 6$ mm implants with bicortical
- 6 anchorage on the bone quantity C $\rightarrow \phi 5 \times 6$ mm implants with bicortical anchorage on the
- 7 bone quantity C, (A) Compressive stress, (B) Tensile stress.